# Cloning, molecular characterization, and expression analysis of a nucleoporin gene (*rgNUP98-96*) from *Rehmannia glutinosa*

**Y.H. Yang[1] and M.J. Li[2]**

[1]College of Bioengineering, Henan University of Technology, Zhengzhou, China
[2]College of Crop Sciences, Fujian Agriculture and Forestry University, Fuzhou, China

Corresponding author: Y.H. Yang
E-mail: yyhui2004@126.com

**ABSTRACT.** Nucleoporin 98 (NUP98) and nucleoporin 96 (NUP96) are essential components of the nuclear pore complex (NPC) in eukaryote cells. However, there is a lack of available information about complete *Rehmannia glutinosa* NUP98-96 (*rgNUP98-96*) sequences. Here, the full-length cDNA sequence of *rgNUP96-98* was isolated from *R. glutinosa* using rapid amplification of cDNA ends (RACE) technology, based on a cloned cDNA sequence (GenBank accession No. JZ483329). The identified *rgNUP98-96* was 3476 bp, and it encoded a 1041-amino acid peptide. The BLAST search analysis of rgNUP98-96 showed an intermediate degree of similarity (60-79%) to the NUP98-96 protein sequences of 34 other plants, including the dicotyledons *Erythranthe guttata*, *Genlisea aurea*, *Coffea canephora*, *Nicotiana benthamiana*, *Solanum lycopersicum,* and *Solanum tuberosum*. The phylogenetic analysis of NUP96-98 sequences indicated that *R. glutinosa* and *E. guttata* sequences shared the closest homology. The calculated molecular mass and predicted isolectric point of the complex protein were 117.6 kDa and 4.99, respectively. The secondary and three-dimensional structure studies illustrated that the rgNUP96-98 protein folded into a channel motif comprised of 34 alpha-helices, nine beta-strands, and

several long loops. Using quantitative real-time PCR, the spatio-temporal expression patterns of *rgNUP98-96* were analyzed in *R. glutinosa*, and the results indicated that *rgNUP98-96* was highly expressed at the early stage of *R. glutinosa* tuberous root expansion, which is associated with a higher expression pattern in roots. The study provides a valuable foundation for further investigation of *rgNUP96-98* molecular functions in *R. glutinosa*.

**Key words:** NUP98-96; *R. glutinosa*; RACE technology; qRT-PCR; Sequence analysis

## INTRODUCTION

The nuclear pore complex (NPC) is the sole gateway between the nucleoplasm and the cytoplasm, reconciling RNA and protein traffic in eukaryotic cells. It is a crucial process for various cellular activities that regulate gene expression, facilitate cell nucleocytoplasmic transport, and influence development (Fiserova et al., 2009; Hetzer and Wente, 2009; Bonnet et al., 2015). Plant NPCs are comprised of multiple copies of approximately 30 different proteins called nucleoporins (Parry, 2013; 2014). Nucleoporin 98 (NUP98; a gatekeeper) and nucleoporin 96 (NUP96; a scaffold), are essential components of the NPC, and are located at both the cytoplasmic and the nuclear sides of the NPC central channel (Terry and Wente 2009; Parrott et al., 2011; Stuwe et al., 2012; Franks and Hetzer, 2013; Byrne et al., 2014; Morchoisne-Bolhy et al., 2015). In many cells, the conserved*NUP98-96*genes generate a long mRNA with an open reading frame (ORF) for a polyprotein. This polyprotein is processed by autocatalytic cleavage that subsequently separates the two functional units (NUP98 and NUP96), which control the transcription of specific target genes that regulate developmental transitions and the cell cycle (Hülsmann et al., 2012; Panda et al., 2015). The composition and function of the NPCs have been well identified and characterized in vertebrate and yeast cells (Tran and Wente, 2006; Aitchison and Rout, 2012), whereas the status of research aimed at deciphering those of the plant NPCs is limited (Tamura et al., 2010; Chang et al., 2013; Tatout et al., 2014). Although *NUP98-96* has been identified and annotated by automated computational analysis for some plant species (e.g., *Arabidopsis*, *Solanum lycopersicum,* and *Glycine max*) (Tamura et al., 2010; Potato Genome Sequencing Consortium, 2011; Chang et al., 2013; Park et al., 2014), there is little information about plant *NUP98-96* isolation and characterization.

*Rehmannia glutinosa* (Scrophulariaceae) is a perennial herbaceous plant. It has various medicinal properties that are associated with its astringent, diuretic, anti-inflammatory, anti-fungal, and anti-radiation characteristics. It is also used in treating liver disorders and diabetes. Because of its specific actions, lack of serious side effects, and lower price, *R. glutinosa* is one of the most popular medicines used in traditional Chinese clinical practice. However, there is currently no information regarding specific *R. glutinosa* molecules or nucleoporins with altered nuclear transport during development processes, and the genomic resources available for *R. glutinosa* are limited (Yang et al., 2013). The rapid amplification of cDNA ends (RACE) technique allows the characterization of the full-length sequence of an RNA transcript found in various tissues, especially those of non-model organisms that lack a full genome sequence (Scotto-Lavino et al., 2006a; 2006b). Here, we described the application of RACE technology to obtain a full-length cDNA encoding *NUP98-96* from *R. glutinosa* (*rgNUP98-96*). We also analyzed the rgNUP98-96 phylogeny and its structural models to present a three-dimensional (3D) structure, which allowed us to recognize its active sites. Finally, we investigated the expression patterns of this gene in various

tissues during *R. glutinosa* development stages. The purpose was to reveal the possible functions of *rgNUP98-96* and their target proteins during the *R. glutinosa* developmental processes.

## MATERIAL AND METHODS

### Plant materials

The *R. glutinosa* cultivar "Wen 85-5" was cultured from the Wen Agricultural Institute, Jiaozuo City, Henan Province, China. The plants were grown between April 22, 2013 and November 30, 2013. To clone gene sequences, a mixture of five whole plants (including leaves, stems, and roots) was sampled at the early stage of *R. glutinosa* tuberous root expansion (July 22, 2013). The roots, stems, and leaves from five independent plants were collected every month from May 22 to October 22, 2013 to measure gene expression patterns during the following developmental stages: seedlings (May 22), root elongation (June 22), tuberous root expansion (early, July 22; middle, August 22; and late, September 22), and maturity (October 22).

### Total RNA extraction, gene cloning, and sequencing

The TriZOL reagent (TaKaRa Co., Tokyo, Japan) was used to extract total RNA from each sample, following the manufacturer protocol. For 5'-RACE and 3'-RACE, the primers (Table 1) were designed according to a 786 bp fragment of *rgNUP98-96* cDNA, which was obtained from *R. glutinosa* EST sequences in GenBank (accession No. JZ483329) at the National Center for Biotechnology Information (NCBI) (http://www.ncbi.nlm.nih.gov/dbEST/). For 3' and 5'-RACE, total RNA was incubated with SMARTScribeTM Reverse Transcriptase (Clontech Laboratories, Inc., USA ) and 3' and 5'-RACE CDS Primer A, respectively. Using touchdown PCR, the first cDNA chain was amplified with an *rgNUP98-96* gene-specific primer for 5' and 3' ends and the Universal Primer A Mix supplied with the kit. Nested PCR was performed with a gene-specific primer for 5' and 3' ends and the short Nested Universal Primer A from the kit. The nested PCR products were separated on a 1.2% (w/v) agarose gel, and each of the target DNAs (5' and 3' ends with the expected size) were then excised from the gel and purified using a MiniBEST Agarose Gel DNA Extraction Kit Ver. 4.0 (TaKaRa Co., Tokyo, Japan). The purified fragments were cloned into the pMD18-T Vector (Takara, Japan) and transformed into *E. coli* DH5α cells. After screening, the recombinant plasmids were isolated and purified, and the target DNA was Sanger sequenced in both directions. The full-length cDNA of the gene was obtained by assembling the partial cDNA and the 5' and 3' ends. Bioinformatic analyses were performed using DNAman software.

**Table 1.** The primer sequences used in R. glutinosa RACE PCR and qRT-PCR analyses.

| PCR Type | | Primer | Sequence (5' to 3') | Site (bp) | Tm (ºC) |
|---|---|---|---|---|---|
| RACE | Touchdown PCR | 5' end | CAAGACACAGCAACTGAGAAACAAATG | 482 | 65.5 |
| | | 3' end | TAGGACTGGTAATGTGGTATCAGCTTC | 180 | 67.1 |
| | Nested PCR | 5' end | CAAGACACAGCAACTGAGAAACAAATG | 34 | 65.6 |
| | | 3' end | ACCTAGCTTATTATCTTATGCTTCTTC | 384 | 62.2 |
| qRT-PCR | | NUP98-96 | Forward: CATAAGACAAATGCCGCTCTCA | 107 | 60.5 |
| | | | Reverse: ATAAACAATGCCGCGTCAAC | 311 | 58.7 |
| | | 18S rRNA* | Forward: TTCTTAGTTGGTGGAGCGATT | 1281 | 58.9 |
| | | | Reverse: CAGACCTGTTATTGCCTCAAAC | 1435 | 59.5 |

*The primers used to amplify the reference gene (18S rRNA) are also listed.

### *rgNUP98-96* sequence analysis and prediction

The obtained nucleotide sequence was translated using Translate Tool (http://www.expasy.ch/tools/translate/), and the properties of the deduced amino acid sequence were estimated using ProtParam (http://web.expasy.org/protparam/). Predictions for isoelectric point (pI) and molecular mass were made using the entire open read frame (ORF) and the pI/MW tool at Expasy (http://web.expasy.org/compute_pi/). The prediction of protein localization sites in cells was conducted using the PSORT program (http://psort.hgc.jp), and the secondary structure was determined using PSIpred (http://bioinf.cs.ucl.ac.uk/psipred/) (Herbert and Bemstein, 2000). The 3D structure of the rgNUP98-96 protein was predicted using the CPHmodles 3.2 server (http://www.cbs.dtu.dk/services/CPHmodels/) and the RasMol program (http://en.wikipedia.org/wiki/RasMol/) (Bernstein, 2000). Conserved domains of the deduced protein sequence were obtained by searching for homologous proteins in different databases using the BLASTp-Basic Local Alignment Search tool at NCBI (http://blast.ncbi.nlm.nih.gov/Blast/). Sequences with the similarities were separated, and multiple alignments and phylogenetic construction were performed using MEGA 4.0 (Kumar et al., 2008).

### Quantitative real-time PCR (qRT-PCR) analysis

Following incubation with RNase-free DNase I, reverse transcription reactions were performed using 5 µg of RNA and M-MLV reverse transcriptase (TaKaRa Co., Tokyo, Japan) in accordance with the manufacturer instructions. For qRT-PCR, the primers were designed based on the *rgNUP98-96* ORF sequences. A primer pair for 18S ribosomal RNA (GenBank ID: EU787015.1) was used as the inner control. Primers were designed using Beacon Designer 7.0 software (Premier Biosoft International, Palo Alto, CA, USA), and the PCR primers are shown in Table 1. To detect gene expression abundances, qRT-PCR reactions were performed using a BIO-RAD iQ5 real-time PCR detection system (Bio-Rad Laboratories, Inc., USA) and Maxima™ SYBR Green qPCR Master Mix (2X) (Fermentas, CanadaCo., Ltd., Canada). The reaction mixture (25 µL) contained 0.5 µM of each primer and the appropriate amounts of enzymes, cDNA, and fluorescent dyes. All runs used a negative control without adding target cDNA, resulting in no detectable fluorescence signal from the reaction. A range of five total cDNA dilutions was tested under the same conditions. Amplification reactions were initiated with a pre-denaturing step at 95ºC for 10 s, which was followed by denaturing (95ºC for 5 s), annealing (59ºC for 10 s), and extension (72ºC for 15 s) steps for 40 cycles during the second stage. A final stage of 55 to 95ºC was used to determine the dissociation curves of the amplified products. All reactions were performed with at least three replicates. The relative expression levels of these genes were calculated using the $2^{-\Delta\Delta CT}$ method, and the data were normalized based on 18S ribosomal RNA CT values (Livak and Schmittgen, 2001).

### RESULTS

### Analysis of nucleotides and deduced amino acids

In order to characterize the full-length *rgNUP98-96* cDNA, total RNA was isolated at the early stage of *R. glutinosa* tuberous root expansion. We designed 5' and 3' cDNA touchdown nested PCR primers based on the EST sequence from NCBI Genbank (accession No. JZ483329). Based on the SMART-RACE technology, 2300 bp of 5' and 1400 bp of 3' *rgNUP98-96* cDNA products were amplified via the touchdown PCR approach (Figure 1a), and approximately 2000

bp and 1200 bp fragments of *rgNUP98-96* 5' and 3' cDNA were isolated using the nested PCR method, respectively (Figure 1b). Nested PCR fragments of the expected size were purified, cloned, transformed, and positively screened. Using Sanger sequencing technology, we obtained 1925 bp and 1201 bp of *rgNUP98-96* cDNA 5' and 3' ends, respectively. After the sequences were assembled using DNAman, a 3476 bp fragment of the *rgNUP98-96* cDNA was generated, containing a 3123 bp coding sequence, which encoded a 1041 amino acid residue protein (Figure 2). Sequence analysis revealed an ATG start codon at a position equivalent to a short (77 bp) 5'-untranslated region (UTR). The framed ATG codon region was also present in the nucleotides at positions +4 (G) and -3 (A), which was a typical KOAZK (AXXATGG) character sequence from the cap that contained TATA-like,CAAT-like, and GC-Box sequenceelements in the 5' upstream UTR. In addition, the 3' downstream UTR existed in an unsteady signal sequence. The results showed that the cDNA was a full-length *NUP98-96* sequence that contained a complete ORF.

The calculated molecular mass of the deduced polypeptide was 117.6 kDa, and the predicted pI was 4.99 (**Table S1**). The total number of negatively (Asp + Glu) and positively (Arg + Lys) charged residues were 157 and 102, respectively. Using the PSORT program, the protein subcellular localization prediction of rgNUP98-96 is in the cell nucleus.
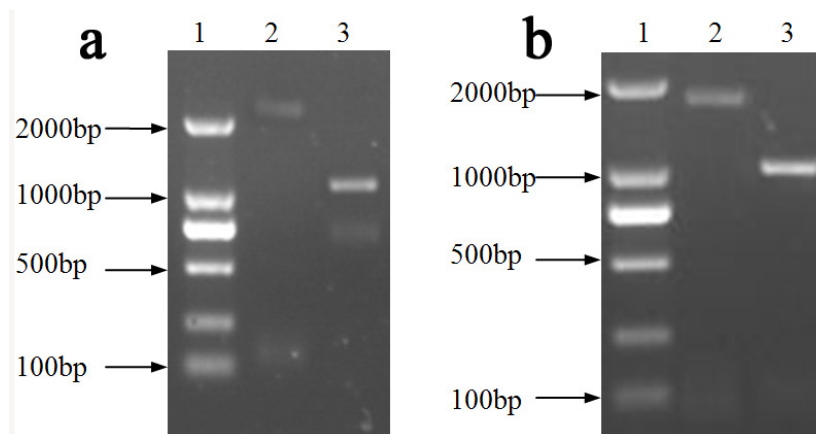


**Figure 1.** Agarose gel electrophoresis of *R. glutinosa* NUP98-96 PCR products using SMARTerTM Race technology. (**a**) Touchdown PCR products. *Lane 1*: DL2000 size marker; *Lane 2*: 5' Race PCR products; *Lane 3*: 3' Race PCR products. (**b**) Nested PCR products. *Lane 1*: DL2000 size marker; *Lane 2*: 5' Race PCR products; *Lane 3*: 3' Race PCR products.

## Analysis of conserved domains and phylogeny

To explain the characteristic features of *rgNUP98-96*, the deduced polypeptide sequence was aligned with the NCBI non-redundant sequences (Nr) database using BLASTp with default parameters. We detected two putative NUP2 (pfam accession: PF04096) and NUP96 (pfam accession: PF12110) conserved domains (Nup2 and Nup96) in Nup98-96. The rgNUP98-96 polypeptide domain exists in the conserved cleavage site (187) between His-Phe-Ser (HFS) within the NUP2 domain, and it produces two nucleoporins, NUP98 (186 aa) and NUP 96 (855 aa) (Figure 2 and **Figure S1**).

The deduced *rgNUP98-96* amino acid sequence showed an intermediate degree of similarity (60-79% identity) with the NUP98-96 sequences from 34 other plant species (Table 2).

To analyze the rgNUP98-96 phylogenetic relationships across plant species, a phylogenetic tree was constructed from an alignment of the rgNUP98-96 deduced amino acid sequence and the sequences from the 34 plant species (Figure 3). As expected, the *NUP98-96* sequences of *R. glutinosa* and six other dicotyledons (*Erythranthe guttata*, *Genlisea aurea*, *Coffea canephora*, *Nicotiana benthamiana*, *Solanum lycopersicum*, and *Solanum tuberosum*), indicated close homology, and the sequence relationships were especially close between *R. glutinosa* and *Erythranthe guttata*.
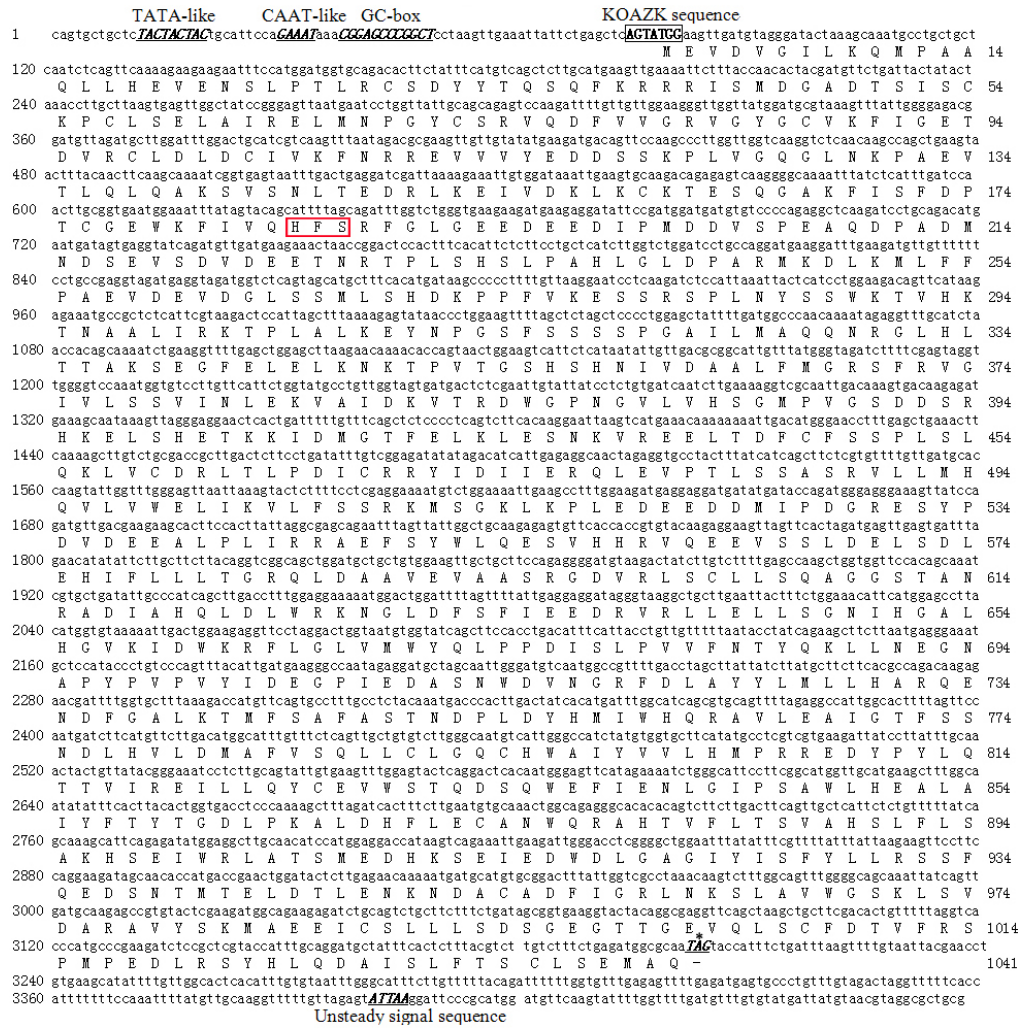


**Figure 2.** Full-length *R. glutinosa* rgNUP98-96 cDNA sequences and deduced amino acids. Note: The cDNA letters and numbers are in black font and those for proteins are in blue font. rgNUP98-96 has three 5'-UTR characters (including TATA-like, CAAT-like, and GC-box sequence fragments) at the beginning of the 5' end cDNA, which are shown in boldface and underlined. The KOAZK sequence around the initiation codon is marked in boldface and is highlighted with a black box. The terminator codon is marked with "*", is shown in boldface and underlined. An unsteady signal sequence (ATTAA) from the 3'-UTR is shown in boldface and underlined. A cleavage motif from the deduced amino acid is highlighted with a red box.

**Table 2.** The rgNUP98-96 gene identity analysis between *R. glutinosa* and other plants.

| Plant species | Total score | Query cover (%) | Identity (%) | Accession |
|---|---|---|---|---|
| *Arabidopsis lyrata* subsp. *lyrata* | 1256 | 98 | 61 | XP_002889279.1 |
| *Arabidopsis thaliana* | 1263 | 98 | 61 | NP_178183.2 |
| *Capsella rubella* | 1247 | 98 | 61 | XP_006300673.1 |
| *Cicer arietinum* | 1265 | 99 | 61 | XP_004491602.1 |
| *Citrus clementina* | 1369 | 98 | 64 | XP_006427580.1 |
| *Citrus sinensis* | 1354 | 98 | 64 | XP_006465209.1 |
| *Coffea canephora* | 1456 | 94 | 72 | CDO98208.1 |
| *Cucumis melo* | 1285 | 98 | 61 | XP_008449614.1 |
| *Cucumis sativus* | 1281 | 99 | 61 | XP_004140177.1 |
| *Eucalyptus grandis* | 1303 | 98 | 63 | KCW70788.1 |
| *Eutrema halophilum* | 1257 | 98 | 61 | BAJ34529.1 |
| *Eutrema salsugineum* | 1259 | 98 | 61 | XP_006389822.1 |
| *Fragaria vesca* subsp. *vesca* | 1274 | 95 | 62 | XP_004301585.1 |
| *Genlisea aurea* | 1317 | 95 | 66 | EPS71530.1 |
| *Glycine max* | 1286 | 99 | 60 | XP_003544079.1 |
| *Jatropha curcas* | 1397 | 98 | 66 | KDP41997.1 |
| *Malus domestica* | 1014 | 65 | 70 | XP_008357609.1 |
| *Medicago truncatula* | 1231 | 99 | 60 | XP_003618002.1 |
| *Erythranthe guttatus* | 1670 | 100 | 79 | EYU21718.1 |
| *Morus notabilis* | 1150 | 85 | 62 | EXB67202.1 |
| *Nicotiana benthamiana* | 1484 | 99 | 69 | BAO49746.1 |
| *Oryza stativa Indica* group | 1113 | 95 | 60 | EAY88730.1 |
| *Oryza stativa Japonica* group | 1108 | 95 | 60 | NP_001049116.1 |
| *Phaseolus vulgaris* | 1276 | 99 | 61 | XP_007142513.1 |
| *Phoenix dactylifera* | 1239 | 98 | 61 | XP_008801016.1 |
| *Prunus mume* | 1365 | 99 | 64 | XP_008232110.1 |
| *Prunus persica* | 1371 | 99 | 64 | XP_007220283.1 |
| *Prunus trichocarpa* | 1365 | 98 | 65 | XP_002303836.1 |
| *Ricinus communis* | 1345 | 99 | 63 | XP_002527319.1 |
| *Solanum lycopersicum* | 1471 | 99 | 69 | XP_006341370.1 |
| *Solanum tuberosum* | 1429 | 99 | 67 | XP_004235924.1 |
| *Theobroma cacao* | 1408 | 98 | 65 | XP_007023385.1 |
| *Vitis vinifera* | 1471 | 98 | 69 | XP_002271967.1 |
| *Zea mays* | 619 | 57 | 60 | XP_008676303.1 |



**Figure 3.** Phylogenetic analysis of the rgNUP98-96 deduced amino acid sequence with the sequences of other plants. The scale over the tree refers to the divergence percentage.

## rgNUP98-96 secondary structure prediction

Secondary structure analysis of the rgNUP98-96 protein by SOMPA and PSIpred programs revealed that it consisted of 34 alpha-helices and nine beta-strands (Figure 4). Using the CPHmodels 3.2 server and the RasMol program, the 3D structure of rgNUP98-96 (Figure 5) was determined using the crystal structure of the C-terminal autoproteolytic domain of the human nucleoporin NUP98 (PDB ID code 1KO6.A) as a template for comparative modeling. An estimated 42.3% identity was calculated between human and *R. glutinosa* NUP98-96 aligned regions (E value = 1e-19). The 3D structure of the rgNUP98-96 protein from front or back views indicated that it roughly folded into similar channel-pore motifs with closely surrounding helices. The 3D structure from left and right views is somewhat similar to a half-open sandwich with some helices.



**Figure 4.** Predicted secondary structure of rgNUP98-96 using the PSIpred program.
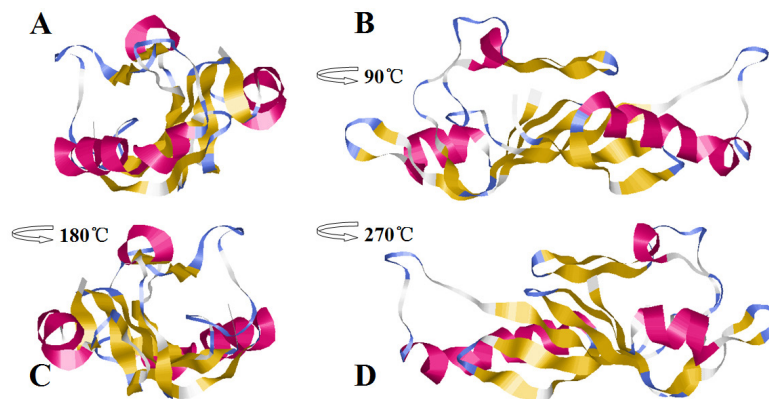


**Figure 5.** Cartoon display of the 3D structure of rgNUP98-96. The front, left, back, and right views are represented as A, B, C, and D, respectively.

## Expression patterns of *rgNUP98-96*

Using qRT-PCR analyses, the expression levels of *rgNUP98-96* were compared between the roots, stems, and leaves of *R. glutinosa* at six different development stages (Figure 6). The results indicated that *rgNUP98-96* displayed some differential expression in the roots, stems, and leaves at the six stages. The accumulation levels of the *rgNup98-96* transcripts in roots were higher than in stems and leaves for three stages of *R. glutinosa* development, and it was strongly transcribed at the early stage of tuberous root expansion. In contrast, there was almost no tissue-specific expression at the seedling, late tuberous root expansion, and maturity stages. Moreover, *rgNUP98-96* is essentially not expressed in tissues during the maturity stage of *R. glutinosa* development.
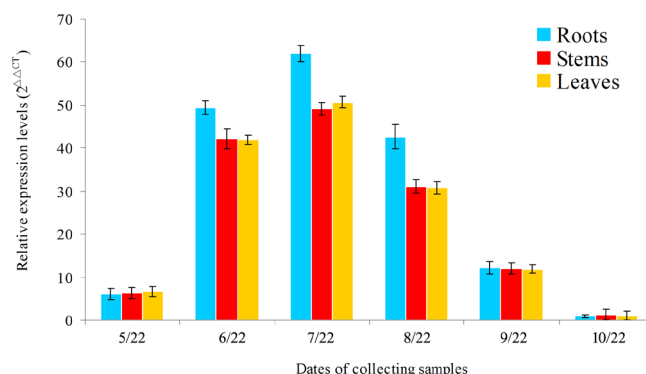


**Figure 6.** Expression patterns of rgNUP98-96 in *R. glutinosa* roots, stems, and leaves at six developmental stages.

## DISCUSSSION

While most plant NUP cDNA sequences were obtained through searching available genomes (Parry, 2013; 2014), few NUP genes from plants without genomes have been characterized by the methods used in this study. Here, due to the lack of an *R. glutinosa* genome (Yang et al., 2013), it was necessary to successfully isolate and characterize *rgNUP98-96* using RACE and bioinformatics technologies.

Previous reports indicated that the aminoacid length of NUP98-96 ranged from approximately 950-1100 aa in other most plant species (Alverson et al., 2011; Motamayor et al., 2013; Mybury et al., 2014). In our study, a 3476 bp cDNA fragment with a 3123 bp ORF was isolated from *R. glutinosa*, which was translated into a 1041 aa with a calculated molecular mass of 117.6 kDa. In many eukaryotic cells, *NUP98-96* is a conservedand long mRNA, and its ORF encodes a polyprotein that is auto-catalytically cleaved at a conserved site that subsequently separates the NUP98 and NUP96 proteins (Iwamoto et al., 2010). In *R. glutinosa*, *rgNUP98-96* was also a single polypeptide gene, which encoded both NUP98 and NUP96 proteins. Another characteristic feature of the rgNUP98-96 protein were conserved auto-cleaved amino acid residues (HFS) in the C-terminal region (187-189 aa) as previously described in most organisms (Mans et al., 2004; Parrott et al., 2011). The secondary structure analysis of the rgNUP98-96 protein indicated high identity with that of the *S. tuberosum* NUP98-96 protein, and the rgNUP98-96 3D structure was highly similar to the human NUP98-96, suggesting that the rgNUP98-96 molecular structure and function might be essential characters of most eukaryotic cells.

Since NUP98 and NUP96 are expressed as a single polypeptide, the amounts of the two nucleoporins in the cell are nearly equivalent. Therefore, we measured the *rgNUP98-96* expression patterns in order to examine its regulation in various tissues and at different development stages of *R. glutinosa*. The results indicated that *rgNUP98-96* expression levels were highest at the early stage of *R. glutinosa* tuberous root expansion. Therefore, the early stage of tuberous root expansion is a key phase, and the gene expression results are in agreement with previous reports (Yang et al., 2013; 2014). Moreover, we found that *rgNUP98-96* expression levels in *R. glutinosa* roots were higher than that in its stems and leaves at three development stages. It has been reported in several plant species that *NUP98-96* products (NUP98 and NUP96) have a variety of specific functions that regulate cell division and differentiation programs (Parrott et al., 2011; Parry, 2014). We hypothesized that higher *rgNUP98-96* expression in *R. glutinosa* roots could be *involved in cellular differentiation and division processes, thus promoting tuberous root expansion.*

Although the details of the mechanisms underlying these processes require considerable experimental validation, this study could shed light to clarify the molecular basis of *rgNUP98-96* functions. In conclusion, the *rgNUP98-96* cDNA characterization succeeded in providing a number of valuable clues to aid in understanding the molecular mechanisms of *R. glutinosa* developmental processes. Furthermore, the findings contribute to the broader understanding of basic NPC molecular structure and function in plants.

## Conflicts of interest

The authors declare no conflict of interest.

## ACKNOWLEDGMENTS

## Supplementary material

## REFERENCES

Aitchison JD and Rout MP (2012). The yeast nuclear pore complex and transport through it. *Genetics* 190: 855-883.

Alverson AJ, Rice DW, Dickinson S, Barry K, et al. (2011). Origins and recombination of the bacterial-sized multichromosomal mitochondrial genome of cucumber. *Plant Cell* 23: 2499-2513.

Bernstein HJ (2000). Recent changes to RasMol, recombining the variants. *Trends Biochem. Sci.* 25: 453-455.

Bonnet A, Bretes H and Palancade B (2015). Nuclear pore components affect distinct stages of intron-containing gene expression. *Nucleic Acids Res.* 43: 4249-4261.

Byrne M, Bennett RL, Cheng X and May WS (2014). Progressive genomic instability in the Nup98-HoxD13 model of MDS correlates with loss of the PIG-A gene product. *Neoplasia* 16: 627-633.

Chang S, Wang Y, Lu J, Gai J, et al. (2013). The mitochondrial genome of soybean reveals complex genome structures and gene evolution at intercellular and phylogenetic levels. *PLoS One* 8: e56502.

Fiserova J, Kiseleva E and Goldberg MW (2009). Nuclear envelope and nuclear pore complex structure and organization in tobacco BY-2 cells. *Plant J.* 59: 243-255.

Franks TM and Hetzer MW (2013). The role of Nup98 in transcription regulation in healthy and diseased cells. *Trends Cell Biol.* 23: 112-117.

Hetzer MW and Wente SR (2009). Border control at the nucleus: biogenesis and organization of the nuclear membrane and pore complexes. *Dev. Cell.* 17: 606-616.

Hülsmann BB, Labokha AA and Görlich D (2012). The permeability of reconstituted nuclear pores provides direct evidence for the selective phase model. *Cell* 150: 738-751.

Iwamoto M, Asakawa H, Hiraoka Y and Haraguchi T (2010). Nucleoporin Nup98: a gatekeeper in the eukaryotic kingdoms. *Genes Cells* 15: 661-669.

Kumar S, Dudley J, Nei M and Tamura K (2008). MEGA: A biologist-centric software for evolutionary analysis of DNA and protein sequences. *Brief. Bioinform.* 9: 299-306.

LivakKJ and SchmittgenTD (2001). Analysis ofrelati vegene expression data using real-time quantitative PCRandthe2 (-DeltaDeltaC(T)). *Method* 25: 402-408.

Mans BJ, Anantharaman V, Aravind L and Koonin EV (2004). Comparative genomics, evolution and origins of the nuclear envelope and nuclear pore complex. *Cell Cycle* 3: 1612-1637.

Morchoisne-Bolhy S, Geoffroy MC, Bouhlel IB, Alves A, et al. (2015). Intranuclear dynamics of the Nup107-160 complex. *Mol. Biol. Cell* 26: 2343-2356.

Motamayor JC, Mockaitis K, Schmutz J, Haiminen N, et al. (2013). The genome sequence of the most widely cultivated cacao type and its use to identify candidate genes regulating pod color. *Genome Biol*. 14: r53.

Panda D, Gold B, Tartell MA, Rausch K, et al. (2015). The transcription factor FoxK participates with Nup98 to regulate antiviral gene expression. *mBio* 6: e02509-14.

Park GT, Frost JM, Park JS, Kim TH, et al. (2014). Nucleoporin MOS7/Nup88 is required for mitosis in gametogenesis and seed development in *Arabidopsis*. *Proc. Natl. Acad. Sci. USA* 111: 18393-18398.

Parrott BB, Chiang Y, Hudson A, Sarkar A, et al. (2011). Nucleoporin98-96 function is required for transit amplification divisions in the germ line of *Drosophila melanogaster*. *PLoS One* 6: e25087.

Parry G (2013). Assessing the function of theplantnuclear pore complexand the search for specificity. *J. Exp. Bot.* 64: 833-845.

Parry G (2014). Components of the *Arabidopsis* nuclear pore complex play multiple diverse roles in control of plant growth. *J. Exp. Bot.* 65: 6057-6067.

Potato Genome Sequencing Consortium (2011). Genome sequence and analysis of the tuber crop potato. *Nature* 475: 189-195.

Scotto-Lavino E, Du G and Frohman MA (2006a). 5' end cDNA amplification using classic RACE. *Nat. Protoc*. 1: 2555-2562.

Scotto-Lavino E, Du G and Frohman MA (2006b). 3' end cDNA amplification using classic RACE. *Nat. Protoc*. 6: 2742-2745.

Stuwe T, von Borzyskowski LS, Davenport AM and Hoelz A (2012). Molecular basis for the anchoring of proto-oncoprotein Nup98 to the cytoplasmic face of the nuclear pore complex. *J. Mol. Biol*. 419: 330-346.

Tamura K, Fukao Y, Iwamoto M, Haraguchi T, et al. (2010). Identification and characterization of nuclear pore complex components in *Arabidopsis thaliana*. *Plant Cell* 22: 4084-4097.

Tatout C, Evans DE, Vanrobays E, Probst AV, et al. (2014). The plant LINC complex at the nuclear envelope. *Chromosome Res.* 22: 241-252.

Terry LJ and Wente SR (2009). Flexible gates: dynamic topologies and functions for FG nucleoporins in nucleocytoplasmic transport. *Eukaryotic Cell* 8: 1814-1827.

Tran EJ and Wente SR (2006). Dynamic nuclear pore complexes: life on the edge. *Cell* 125: 1041-1053.

Yang YH, Li MJ, Chen XJ, Wang PF, et al. (2014). *De novo* characterization of the *Rehmannia glutinosa* leaf transcriptome and analysis of gene expression associated with replanting disease. *Mol. Breeding* 34: 905-915.

Yang YH, Zhang ZY, Fan HM, Zhao YD, et al. (2013). Construction and analysis of a different expression cDNA library in *Rehmannia glutinosa* plants subjected to continuous cropping. *Acta Physiol. Plant* 35: 645-655.